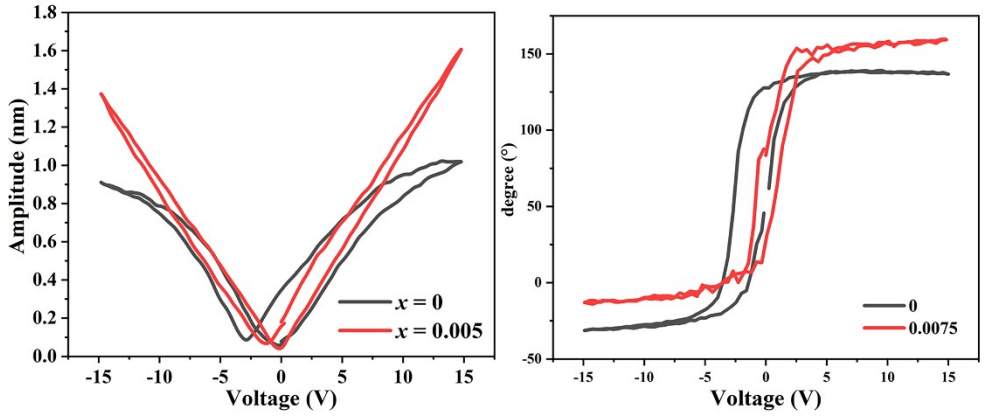

Figure.S1. SS-PFM curves. (a) The butterfly-shaped amplitude loops; (b) the phase loops

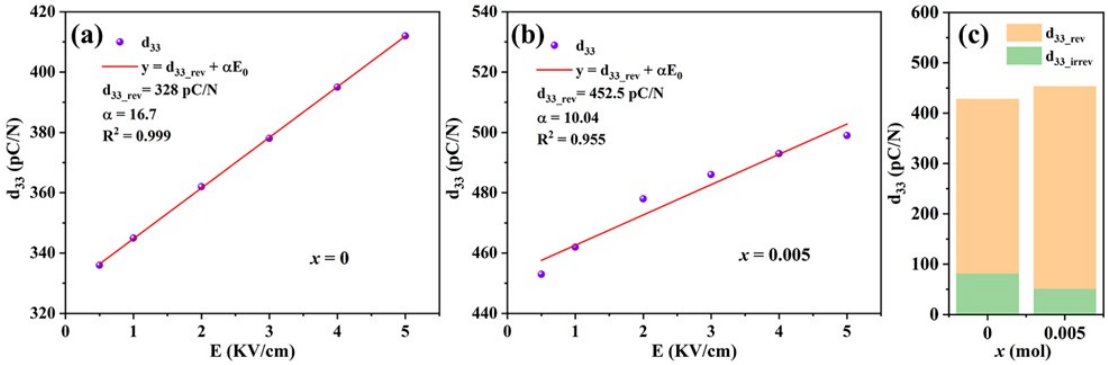

Figure S2. Rayleigh fitting curve of (a) x = 0; (b) x = 0.0075; (c) Piezoelectric contribution calculation for d_{33}_rev and d_{33}_irrev.

Phase field simulation

We employed Phase-field simulations to simulate the microstructure evolution under stress temperature field of samples with compositions x = 0 and x = 0.005. The size of the simulation model is 1000×600 nm^2, and the total free energy includes the following terms:

$$F = \int_V \left(f_{bulk} + f_{grad} + f_{elas} + f_{elec}\right)dV + \int_V f_{localelec}dV \quad (1)$$

$$f_{bulk} = \alpha_1\left(p_1^2 + p_2^2 + p_3^2\right) + \alpha_{11}\left(p_1^2 + p_2^2 + p_3^2\right)^2 + \alpha_{111}\left(p_1^2 + p_2^2 + p_3^2\right)^3 + \left(p_1^2p_2^2 + \alpha_{112}\left(p_1^4p_2^2 + p_2^4p_3^2 + p_1^4p_3^2 + p_1^4p_2^2 + p_1^2p_2^4 + p_2^2p_3^4 + p_1^2p_3^4\right) + \alpha_{113}(p_1^2 p_2^2p_3^2)\right) \quad (2)$$

Where the term f_{bulk} in E_q. (1) describes the bulk free energy density, expressed by Landau's free energy term in E_q. (2). α_1, α_{11}, α_{12} are Landau coefficients depending on

defect concentration c and temperature T. α_{111}, α_{112}, α_{113} are constant coefficients. It should be noticed that the multiple terms in E_q. (2) decide the stability of ferroelectric phases (R, T, O, or C) and barriers between different ferroelectric phases. The global field effect f_{grad} can be described by the associated coefficients referred [1-3].The f_{elas} reflects the long-range elastic interaction energy. The last term $f_{localelec}$ in E_q. (1) represents the local field effect caused by doped defects.

The temporal evolution of the domain structure can be obtained by solving the time-dependent Ginzburg-Landau (TDGL) function as Eq. (3)

$$\frac{dP_i(x,t)}{dt} = -M\frac{\delta F}{\delta P_i(x,t)}, i = 1, 2, 3 \quad (3)$$

where M is the kinetic coefficient related to the domain mobility and t is time. Further mathematical transformation was employed to obtain the symmetry contours from the calculated vector maps. The corresponding simulation results are presented in Fig. 5 (h).

[1] J. Gao, X. Hu, Y. Liu, Y. Wang, X. Ke, D. Wang, L. Zhong and X. Ren, J. Phys. Chem. C, 2017, 121, 2243-2250.

[2] J. Gao, Y. Dai, X. Hu, X. Ke, L. Zhong, S. Li, L. Zhang, Y. Wang, D. Wang and Y. Wang, EPL, 2016, 115, 37001.

[3] X. Hu, J. Gao, Y. Wang, Y. Liu, L. Li, D. Wang, F. Li, R. Yao, L. Zhong and X. Ren, J. Phys. Chem. C, 2019, 123, 15434-15440.